Signaling Architectures that Transmit Unidirectional Information Despite Retroactivity

Citation: Shah, Rushina, and Domitilla Del Vecchio. "Signaling Architectures That Transmit Unidirectional Information Despite Retroactivity." Biophysical Journal 113, no. 3 (August 2017): 728–742. © 2017 Biophysical Society

As Published: http://dx.doi.org/10.1016/J.BPJ.2017.06.019

Publisher: Elsevier

Persistent URL: http://hdl.handle.net/1721.1/119138

Version: Final published version: final published article, as it appeared in a journal, conference proceedings, or other formally published context

Biophysical Journal
Article

Biophysical Society

Signaling Architectures that Transmit Unidirectional Information Despite Retroactivity

Rushina Shah[1,*] and Domitilla Del Vecchio[1]
[1]Department of Mechanical Engineering, Massachusetts Institute of Technology, Cambridge, Massachusetts

ABSTRACT A signaling pathway transmits information from an upstream system to downstream systems, ideally in a unidirectional fashion. A key obstacle to unidirectional transmission is retroactivity, the additional reaction flux that affects a system once its species interact with those of downstream systems. This raises the fundamental question of whether signaling pathways have developed specialized architectures that overcome retroactivity and transmit unidirectional signals. Here, we propose a general procedure based on mathematical analysis that provides an answer to this question. Using this procedure, we analyze the ability of a variety of signaling architectures to transmit one-way (from upstream to downstream) signals, as key biological parameters are tuned. We find that single stage phosphorylation and phosphotransfer systems that transmit signals from a kinase show a stringent design tradeoff that hampers their ability to overcome retroactivity. Interestingly, cascades of these architectures, which are highly represented in nature, can overcome this tradeoff and thus enable unidirectional transmission. By contrast, phosphotransfer systems, and single and double phosphorylation cycles that transmit signals from a substrate, are unable to mitigate retroactivity effects, even when cascaded, and hence are not well suited for unidirectional information transmission. These results are largely independent of the specific reaction-rate constant values, and depend on the topology of the architectures. Our results therefore identify signaling architectures that, allowing unidirectional transmission of signals, embody modular processes that conserve their input/output behavior across multiple contexts. These findings can be used to decompose natural signal transduction networks into modules, and at the same time, they establish a library of devices that can be used in synthetic biology to facilitate modular circuit design.

INTRODUCTION

Cellular signal transduction is typically viewed as a unidirectional transmission of information via biochemical reactions from an upstream system to multiple downstream systems through signaling pathways (1–7). However, without the presence of specialized mechanisms, signal transmission via chemical reactions is not in general unidirectional. In fact, the chemical reactions that allow a signal to be transmitted from an upstream system to downstream systems also affect the upstream system due to the resulting reaction flux. This flux is called retroactivity, which is one of the chief hurdles to one-way transmission of information (8–13). Signaling pathways, typically composed of phosphorylation, dephosphorylation, and phosphotransfer reactions, are highly conserved evolutionarily, such as the MAPK cascade (14) and two-component signaling systems (15). Thus, the same pathways act between different upstream and downstream systems in different scenarios and organisms, facing different effects of retroactivity in different contexts. For signal transmission to be unidirectional in these different contexts, a signaling pathway should have evolved architectures that overcome retroactivity. Specifically, these architectures should impart a small retroactivity to their upstream system (called retroactivity to the input) and should be minimally affected by the retroactivity imparted to them by their downstream systems (retroactivity to the output).

Phosphorylation-dephosphorylation (PD) cycles, phosphotransfer reactions, and cascades of these are ubiquitous in both prokaryotic and eukaryotic signaling pathways, playing a major role in cell cycle progression, survival, growth, differentiation and apoptosis (1–7,16–19). Numerous studies have been conducted to analyze such systems, starting with milestone works by Stadtman and Chock (20–22) and Goldbeter et al. (23–25), which theoretically and experimentally analyzed phosphorylation cycles and cascades. These systems were further investigated by Kholodenko et al. (26–28) and Gomez-Uribe et al. (29,30). However, these studies considered signaling cycles in isolation, and thus did not investigate the effect of retroactivity.

Submitted February 21, 2017, and accepted for publication June 6, 2017.
*Correspondence: rushina@mit.edu
Editor: Reka Albert.
http://dx.doi.org/10.1016/j.bpj.2017.06.019

The effect of retroactivity on such systems was theoretically analyzed in the work by Ventura et al. (31), where retroactivity is treated as a "hidden feedback" to the upstream system. Experimental studies then confirmed the effects of retroactivity in signaling systems through in vivo experiments on the MAPK cascade (12,13) and in vitro experiments on reconstituted covalent modification cycles (9,11). These studies clearly demonstrated that the effects of retroactivity on a signaling system manifest themselves in two ways. They cause a slowdown of the temporal response of the signaling system's output to its input and lead to a change of the output's steady state.

In 2008, Del Vecchio et al. (8) demonstrated theoretically that a single PD cycle with a slow input kinase can attenuate the effect of retroactivity to the output when the total substrate and phosphatase concentrations of the cycle are increased together. Essentially, a sufficiently large phosphatase concentration along with relatively large kinetic rates of modification adjusts the cycle's internal dynamics very quickly with respect to a relatively slower input, making any retroactivity-induced delays negligible on the timescale of the signal being transmitted (32). A similarly large concentration of the total cycle's substrate ensures that the output's steady state is not significantly affected by the presence of downstream sites. These theoretical findings were later verified experimentally both in vitro (11) and in vivo (33). Although a single PD cycle can attenuate the effect of retroactivity to the output, it is unfortunately unsuitable for unidirectional signal transmission. In fact, as the substrate concentration is increased, the PD cycle applies a large retroactivity to the input, causing the input signal to slow down. This was experimentally observed in (33). The experimental results of (34) further suggest that a cascade composed of two PD cycles and a phosphotransfer reaction could overcome both retroactivity to the input and retroactivity to the output. In (35), it was theoretically found that for certain parameter conditions, a cascade of PD cycles could attenuate the upward (from downstream to upstream) propagation of disturbances applied downstream of the cascade. In (36), a parametric study was performed on a cascade of single phosphorylation cycles at steady state, and parametric regimes in which the cascade would transmit signals either upstream (using retroactivity) or downstream were numerically determined. These results suggest that specific signaling architectures may be able to counteract retroactivity. However, to the best of the authors' knowledge, no attempt has been made to systematically characterize signaling architectures with respect to their ability to overcome the effects of retroactivity and therefore enable unidirectional signal transmission.

This work presents a procedure by which to identify and characterize signaling architectures that can transmit unidirectional signals. We first model a general signaling system based on the underlying reactions that the species of the signaling system participate in. These reactions result in an ordinary differential equation (ODE) model based on the reaction-rate equations. Based on this general model, we propose a procedure to evaluate the unidirectional signaling ability of a general signaling architecture that operates on a fast timescale relative to its input. Such a model is valid for many signaling systems that transmit relatively slower signals, such as those from slowly varying "clock" proteins that operate on the timescale of the circadian rhythm (37), from proteins signaling nutrient availability (38), or from proteins whose concentration is regulated by transcriptional networks, which operate on the slower timescale of gene expression (39). Our framework provides expressions for retroactivity to the input and to the output, as well as the input-output relationship of the signaling system. These expressions are given in terms of the reaction-rate parameters and protein concentrations. Based on these expressions, we present a procedure to analyze the ability of signaling systems to transmit unidirectional signals by tuning their total (modified + unmodified) protein concentrations. We focus on total protein concentrations as a design parameter, because these appear to be highly variable in natural systems and through the course of evolution. Thus, it is possible that natural systems themselves use protein concentrations as a design parameter, optimizing them to improve systems' performance (40,41). Further, protein concentrations are also an easily tunable quantity in synthetic genetic circuits. The different "dials" that can be used to tune protein concentration have been characterized in (42). Protein concentrations have been tuned in (33) and (34) to show the effect of increasing substrate and phosphatase concentrations on the retroactivity attenuation properties of a signaling cycle. Thus, we analyze a number of signaling architectures composed of PD cycles and phosphotransfer systems by tuning total protein concentrations.

METHODS

Problem definition

In this work, we consider a general signaling system, **S**, connected between an upstream and downstream system, as shown in Fig. 1 *A*. Here, $\underline{X}$ is the state-variable vector of **S**, and each component of $\underline{X}$ represents the concentration of a species of system **S**. System **S** receives an input from the upstream system in the form of a protein whose concentration is U, and sends an output to the downstream system in the form of a protein whose concentration is Y. When this output protein reacts with the species of the downstream system, whose normalized concentrations are represented by state variable v, the resulting reaction flux changes the behavior of the upstream system. We represent this reaction flux as an additional input, $\mathcal{S}$, to the signaling system. Similarly, when the input protein from the upstream system reacts with the species of the signaling system, the resulting reaction flux changes the behavior of the upstream system. We represent this as an input, $\mathcal{R}$, to the upstream system. We call $\mathcal{R}$ the retroactivity to the input of **S** and $\mathcal{S}$ the retroactivity to the output of **S**, as in (8). For system **S** to transmit a unidirectional signal, the effects of $\mathcal{R}$ on the upstream system and of $\mathcal{S}$ on the downstream system must be small. Retroactivity to the input $\mathcal{R}$ changes the input from U_{ideal} to U, where U_{ideal} is shown in Fig. 1 *B*. Thus, for the effect of $\mathcal{R}$ to be small, the difference between U and U_{ideal} must be small.

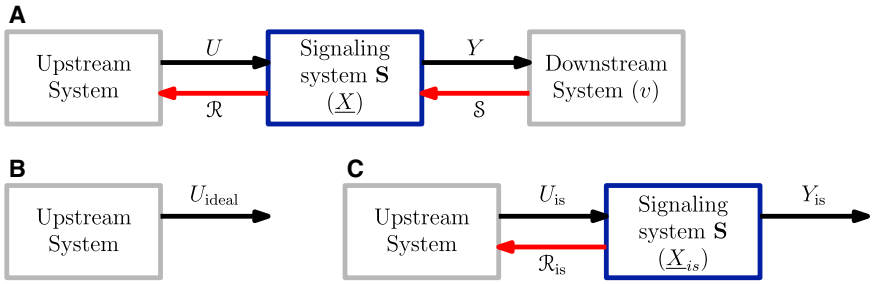

FIGURE 1 Interconnections between signaling system **S** and its upstream and downstream systems, along with input, output, and retroactivity signals. (*A*) Full system showing all interconnection signals: $U(t)$ is the input from the upstream system to the signaling system, with state variable vector $\underline{X}$. $Y(t)$ is the output of the signaling system, sent to the downstream system, whose state variable is v. $\mathcal{R}$ is the retroactivity signal from the signaling system to the upstream system (retroactivity to the input of **S**), and $\mathcal{S}$ is the retroactivity signal from the downstream system to the signaling system (retroactivity to the output of **S**). (*B*) Ideal input, U_{ideal}: output of the upstream system in the absence of the signaling system ($\mathcal{R}=0$). (*C*) Isolated output, Y_{is}: output of the signaling system in the absence of the downstream system ($\mathcal{S}=0$). $\underline{X}_{\text{is}}$ denotes the corresponding state of **S**. To see this figure in color, go online.

Retroactivity to the output $\mathcal{S}$ changes the output from Y_{is} (where "is" stands for isolated) to Y, where Y_{is} is shown in Fig. 1 *C*, and for the effect of retroactivity to the output to be small, the difference between Y_{is} and Y must be small. An ideal unidirectional signaling system is therefore a system where the input U_{ideal} is transmitted from the upstream system to the signaling system without any change imparted by the latter, and the output Y_{is} of the signaling system is also transmitted to the downstream system without any change imparted to it by the downstream system. Based on this concept of ideal unidirectional signaling system, we then present the following definition of a signaling system that can transmit information unidirectionally. To give this definition, we assume that the proteins (besides the input species) that compose signaling system **S** are constitutively produced and therefore their total concentrations (modified and unmodified) are constant. The vector of these total protein concentrations is denoted by $\underline{\Theta}$.

Definition 1

We will say that system **S** is a signaling system that can transmit unidirectional signals for all inputs $U\in[0,U_b]$, if $\underline{\Theta}$ can be chosen such that the following properties are satisfied:

1. $\mathcal{R}$ is small: this is mathematically characterized by requiring that $|U_{\text{ideal}}(t)-U(t)|$ be small for all $U\in[0,U_b]$.
2. System **S** attenuates the effect of $\mathcal{S}$ on Y: this is mathematically characterized by requiring that $|Y_{\text{is}}(t)-Y(t)|$ be small for all $U\in[0,U_b]$.
3. Input-output relationship: $Y_{\text{is}}(t)\approx KU_{\text{is}}(t)^m$, for some $m\geq 1$, for some $K>0$, and for all $U\in[0,U_b]$.

Note that definition 1 specifies that the signaling system must impart a small retroactivity to its input (requirement 1) and attenuate retroactivity to its output (requirement 2). Requirement 3 specifies that the output must not saturate with respect to the input, so that the signal is still propagated downstream by the signaling system. In particular, definition 1 specifies that these properties should be satisfied for a full range of inputs and outputs, implying that these properties must be guaranteed by the features of the signaling system and cannot be enforced by tuning the amplitudes of inputs and/or outputs.

Example

As an illustrative example of the effects of $\mathcal{R}$ and $\mathcal{S}$ on a signaling architecture, we consider a signaling system, **S**, composed of a single PD cycle (8,11,33). The system is shown in Fig. 2 *A*. It receives a slowly varying input signal, U, in the form of kinase concentration Z generated by an upstream system, and it has as the output signal Y the concentration of X^*, which in this example is a transcription factor that binds to promoter sites in the downstream system. Kinase Z phosphorylates protein X to form X^*, which is dephosphorylated by phosphatase M back to X. The state variables $\underline{X}$ of **S** are the concentrations of the species in the cycle, that is, X, M, X^*, C_1, C_2, where C_1 and C_2 are the complexes formed by X and Z during phosphorylation, and by X^* and M during dephosphorylation, respectively. The state variable v of the downstream system is the normalized concentration of C, the complex formed by X* and p (i.e., $v=(C/p_{\text{T}})$ where p_{T} is the total concentration of the downstream promoters). This configuration, where a signaling system has as downstream system(s) gene expression processes, is common in many organisms, as it is often the case that a transcription factor goes through some form of covalent modification before activating or repressing gene expression (43). However, the downstream system could be any other system, such as another covalent modification process, which interacts with the output through a binding-unbinding reaction. We denote the total amount of cycle substrate by $X_T=X+X^*+C_1+C_2+C$ and the total amount of phosphatase by $M_{\text{T}}=M+C_2$.

According to definition 1, we vary the total protein concentrations of the cycle, $\underline{\Theta}=[X_{\text{T}},M_{\text{T}}]$, to investigate the ability of this system to transmit unidirectional signals. To this end, we consider two extreme cases: first, when the total substrate concentration, X_{T}, is low (simulation results in Fig. 2, *B* and *C*), and second, when it is high (simulation results in Fig. 2, *D* and *E*). For both these cases, we change M_{T} proportionally to X_{T}. This is because, for large Michaelis-Menten constants, we have an input-output relationship with $m=1$ and $K\approx(k_1K_{m2}/k_2K_{m1})(X_{\text{T}}/M_{\text{T}})$ (details in Supporting Material, Eq. 21, as defined in Definition 1, requirement 3). To maintain the same K for fair comparison between the two cases, we vary M_{T} proportionally with X_{T}. Here, K_{m1} and k_1 are the Michaelis-Menten constant and catalytic rate constant for the phosphorylation reaction, and K_{m2} and k_2 are the Michaelis-Menten constant and catalytic rate constant for the dephosphorylation reaction. These reactions are shown in Supporting Material, Eq. 16. For the simulation results, we consider a sinusoidal input to see the dynamic response of the system to a time-varying signal. Results for responses to the step input are shown in Fig. S1. For these two cases, then, we see from Fig. 2 *B* (and Fig. S1 *B*) that when X_{T} (and M_{T}) is low, $\mathcal{R}$ is small, i.e., $|U_{\text{ideal}}(t)-U(t)|$ is small (satisfying requirement 1 of definition 1). This is because kinase Z must phosphorylate very little substrate X, and thus, the reaction flux due to phosphorylation to the upstream system is small. However, as seen in Fig. 2 *C* (and Fig. S1 *C*), for low X_{T}, the signaling system is unable to attenuate $\mathcal{S}$. The difference $|X^*_{\text{is}}-X^*|$ is large, and requirement 2 of definition 1 is not satisfied for low X_{T}. This large retroactivity to the output is due to the reduction in the total substrate available for the cycle because of the sequestration of X* by the promoter sites in the downstream system. Since X_{T} is low, this sequestration results in a large relative change in the amount of total substrate available for the cycle, and thus, interconnection to the downstream system has a large effect on the behavior of the cycle. For the case when X_{T} (and M_{T}) is high, the system shows exactly the opposite behavior. From Fig. 2 *D* (and Fig. S1 *D*), we see that $\mathcal{R}$ is high (thus not satisfying requirement 1 of definition 1), since the kinase must phosphorylate a large amount of substrate, but $\mathcal{S}$ is attenuated (satisfying requirement 2), since

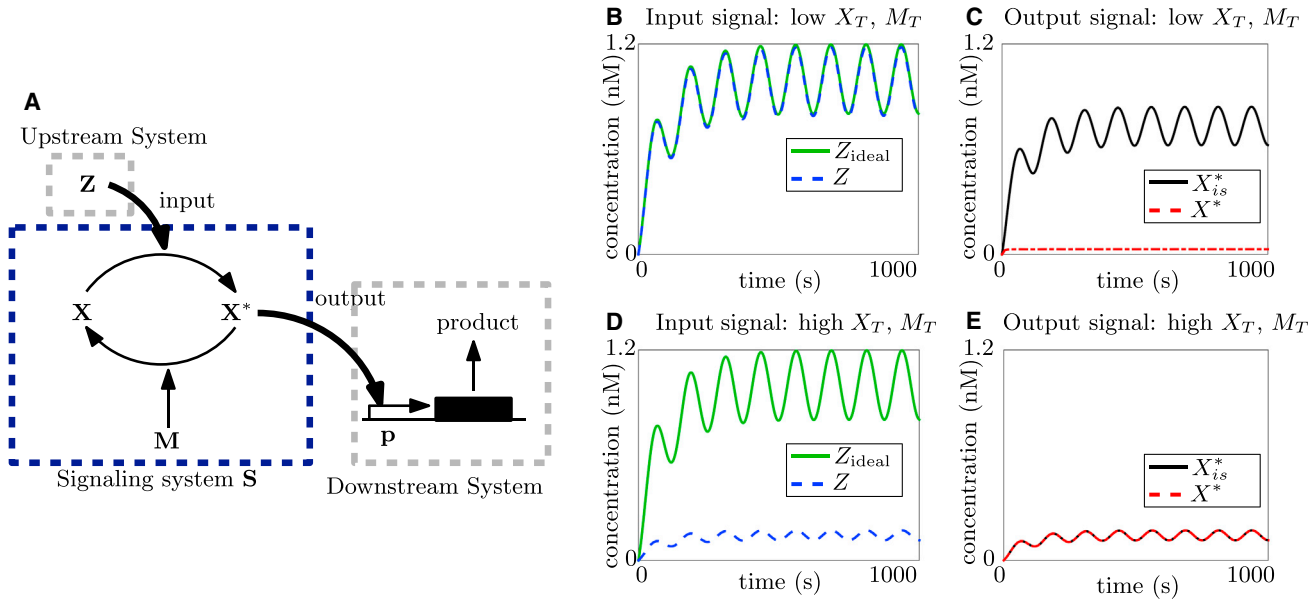

FIGURE 2 Tradeoff between small retroactivity to the input and attenuation of retroactivity to the output in a single phosphorylation cycle. (*A*) Single phosphorylation cycle, with input Z as the kinase: *X* is phosphorylated by Z to *X** and dephosphorylated by the phosphatase *M*. *X** is the output and acts on sites *p* in the downstream system, which is depicted as a gene expression system here. (*B–E*) Simulation results for the ODE model shown in Supporting Material, Eq. 17. Simulation parameters are given in Table S1. The ideal system is simulated for Z_{ideal} with $X_T = M_T = p_T = 0$. The isolated system is simulated for X^*_{is} with $p_T = 0$. To see this figure in color, go online.

there is enough total substrate available for the cycle even once *X** is sequestered. Thus, this system shows a tradeoff: by increasing X_T (and M_T), we attenuate retroactivity to the output but do so at the cost of increasing retroactivity to the input. Similarly, by decreasing X_T (and M_T), we make retroactivity to the input smaller, but at the cost of being unable to attenuate retroactivity to the output. Therefore, requirements 1 and 2 cannot be independently obtained by tuning X_T and M_T.

We note that because the signaling reactions, i.e., phosphorylation and dephosphorylation, act on a faster timescale than the input, the signaling system operates at quasi-steady state and the output is able to quickly catch up to changes in the input. It has been demonstrated in (32,34) that this fast timescale of operation of the signaling system attenuates the temporal effects of retroactivity to the output, which would otherwise result in the output slowing down in the presence of the downstream system. Thus, although the high substrate concentration X_T is required to reduce the effect of retroactivity to the output due to permanent sequestration, timescale separation is necessary for attenuating the temporal effects of the binding-unbinding reaction flux (32).

Generalized model

Although the single phosphorylation cycle shows some ability to attenuate retroactivity, it is not able to transmit unidirectional signals due to the tradeoff seen above. We therefore study different architectures of signaling systems, composed of phosphorylation cycles and phosphotransfer systems that are ubiquitous in natural signal transduction (1–7,14–19). All reactions are modeled as two-step reactions. Phosphorylation and dephosphorylation reactions proceed by first reversibly forming an intermediate complex, which then irreversibly decomposes into the enzyme and the product. Phosphotransfer reactions are modeled as reversible two-step reactions resulting in the transfer of the phosphate group via the formation of an intermediate complex. Based on these reactions, as well as production and decay of the various species, ODE models are created for the systems using reaction-rate equations. Reactions for each system analyzed and the corresponding reaction-rate equation models are shown in Supporting Material, Sections 1.3–1.10. The following general ODE model then describes any signaling system architecture in the interconnection topology of Fig. 1 *A*:

$$\begin{aligned}
\frac{dU}{dt} &= f_0(U, R\underline{X}, S_1 v, t) + G_1 A \underline{r}(U, \underline{X}, S_2 v),\\
\frac{d\underline{X}}{dt} &= G_1 B \underline{r}(U, \underline{X}, S_2 v) + G_1 f_1(U, \underline{X}, S_3 v) + G_2 C s(\underline{X}, v),\\
\frac{dv}{dt} &= G_2 D s(\underline{X}, v),\\
Y &= I\underline{X},
\end{aligned} \tag{1}$$

where, the variable *t* represents time, *U* is the input signal (the concentration of the input species), $\underline{X}$ is a vector of concentrations of the species of the signaling system, *Y* is the output signal (the concentration of the output species) and *v* is the state variable of the downstream system. In the cases that follow, *v* is the normalized concentration of the complex formed by the output species *Y* and its target binding sites *p* in the downstream system.

The internal dynamics of the upstream system are captured by the reaction-rate vector f_0. This vector includes the production and decay terms for the input species. The internal dynamics of the signaling system are captured by the reaction-rate vector f_1. This vector captures the reactions that occur between different species within the signaling system. The reaction-rate vector $\underline{r}$ is the reaction flux resulting from the reactions between species of the upstream system and those of the signaling system. Thus, this vector affects the rate of change of both the input species and the species of the signaling system, with corresponding stoichiometry matrices *A* and *B*. The reaction-rate vector *s* represents the additional reaction flux due to the binding-unbinding of the output protein with the target sites in the downstream system. This vector therefore affects the rate of change of the downstream species as well as the signaling system, with corresponding stoichiometric matrices *C* and *D*. These additional reaction fluxes, $\underline{r}$ and *s*,

affect the temporal behavior of the input and the output, often slowing them down, as demonstrated previously (11).

The parameter R accounts for decay/degradation of complexes formed by the input species with species of the signaling system, thus leading to an additional channel for removal of the input species through their interaction with the signaling system. Similarly, scalar S_1 represents decay of complexes formed by the input species with species of the downstream system. This additional decay leads to an effective increase in decay of the input, thus affecting its steady-state. As species of the signaling system are sequestered by the downstream system, their free concentrations change. This is accounted for by the vectors S_2 and S_3.

The retroactivity to the input $\mathcal{R}$ indicated in Fig. 1 *A* therefore equals $(R, \underline{r}, S_1)$, which leads to both steady-state and temporal effects on the input response. The retroactivity to the output $\mathcal{S}$ of Fig. 1 *A* equals (S_1, S_2, S_3, s), which leads to an effect on the output response. For ideal unidirectional signal transmission, the effects of $\mathcal{R}$ and $\mathcal{S}$ must be small. The ideal input of Fig. 1 *B*, U_{ideal}, is the input when retroactivity to the input $\mathcal{R}$ is zero, i.e., when $R = S_1 = \underline{r} = 0$. The isolated output of Fig. 1 *C*, Y_{is}, is the output when retroactivity to the output $\mathcal{S}$ is zero, i.e., when $S_1 = S_2 = S_3 = s = 0$.

The positive scalar G_1 captures the timescale separation between the reactions of the signaling system and the dynamics of the input. Since we consider relatively slow inputs, we have $G_1 \gg 1$. The positive scalar G_2 captures the timescale separation between the binding-unbinding rates between the output Y and its target sites p in the downstream system and the dynamics of the input. Since binding-unbinding reactions also operate on a fast timescale, we have $G_2 \gg 1$. We define $\epsilon = \max((1/G_1), (1/G_2))$ and thus, $\epsilon \ll 1$. This allows us to apply techniques from singular perturbation to simplify and the set of equations in (1), to arrive at the results presented in the next section. Details of this analysis are shown in Supporting Material, Section 1.1.

In Results, we outline a procedure to determine whether a given signaling system satisfies definition 1. For this, we introduce the following definitions. We assume that there exist matrices M and P, and invertible matrices T and Q such that

$$TA + MB = 0, \quad Mf_1 = 0 \text{ and } QC + PD = 0. \tag{2}$$

This assumption is usually satisfied in signaling systems (32). Further, we have

$$v = \phi(\underline{X}) \text{is the solution to } s(\underline{X}, v) = 0, \tag{3}$$

and

$$\underline{X} = \underline{\Gamma}(U) \text{is the solution to } B\underline{r}(U, \underline{X}, S_2 v) + f_1(U, \underline{X}, S_3 v) = s(\underline{X}, v) = 0. \tag{4}$$

We note that, for system 1 (Supporting Material, Section 1.1), terms S_2 and S_3 and functions f_1 and $\underline{\Gamma}$ depend on the vector of total protein concentrations, $\underline{\Theta}$.

Simulations and validity of results

For most systems, we have assumed that the Michaelis-Menten constants for the phosphorylation and dephosphorylation reactions are larger than protein concentrations. More specific assumptions are stated in Results. Our theoretical analysis for the various systems is valid for all reaction-rate parameters as long as these assumptions are satisfied. Thus, although the simulation results are performed for specific parameters, the conclusions are robust to changes in these parameters. Simulations of the full ODE systems are run on MATLAB, using the numerical ODE solvers ode23s and ode15s. All simulation parameters are picked from the biologically relevant ranges given in (35), and are listed in Table S1.

RESULTS

The main result of this study is twofold. First, we provide a general procedure to determine whether any given signaling system enables unidirectional signal transmission. Second, using this procedure, we analyze the unidirectional signal transmission ability of both common and less frequent signaling architectures. In particular, we found that most signaling architectures transmit information via kinases. Therefore, we have analyzed several architectures where this is the case. However, both nature and a human designer have the option of designing a system that would transmit information via substrates. Since this is not frequently encountered in natural signaling architectures, we analyzed whether these designs show a disadvantage to unidirectional signaling, as indeed we find they do.

Procedure to determine unidirectional signal transmission

We outline a procedure to determine whether any given signaling system can enable unidirectional signaling in Fig. 3. First, the reaction-rate equations of the signaling system are written in form (1) (Supporting Material, Section 1.1), allowing us to note the terms S_1, S_2, S_3, and R for step 2. The remaining terms for step 2 are computed using Eqs. 2–4 under Generalized model. The terms in steps 3–5 are computed using the terms in step 2. The upper bound on $|U(t) - U_{\text{ideal}}(t)|$ is proportional to the terms found in step 3, and thus, as these are made small according to test (i), the first requirement of definition 1 is satisfied. The analysis giving rise to these terms is shown in theorem 1 in Supporting Material, Section 1.1. Similarly, the upper bound on $|Y_{\text{is}}(t) - Y(t)|$ is proportional to the terms in step 4, and thus, as these are made small according to test (ii), the second requirement of definition 1 is satisfied. This is derived in theorem 2 in Supporting Material, Section 1.1. Theorem 3 in Supporting Material, Section 1.1 shows that the input-output relationship for the signaling system can be computed by step 5. If this input-output relationship satisfies test (iii), the third requirement of definition 1 is satisfied. Once tests (i)–(iii) are satisfied, test (iv) checks whether all the requirements for definition 1 can be achieved simultaneously by tuning $\underline{\Theta}$. If this is possible, the signaling system is said to be able to transmit a unidirectional signal.

Note that throughout this work, $\underline{\Theta}$ is assumed to be the design parameter, since it is relatively easier to tune in both natural and synthetic circuits. However, the procedure outlined in Fig. 3 holds even if different design parameters are chosen.

As an example of the application of the procedure, we consider once again the single PD cycle (see

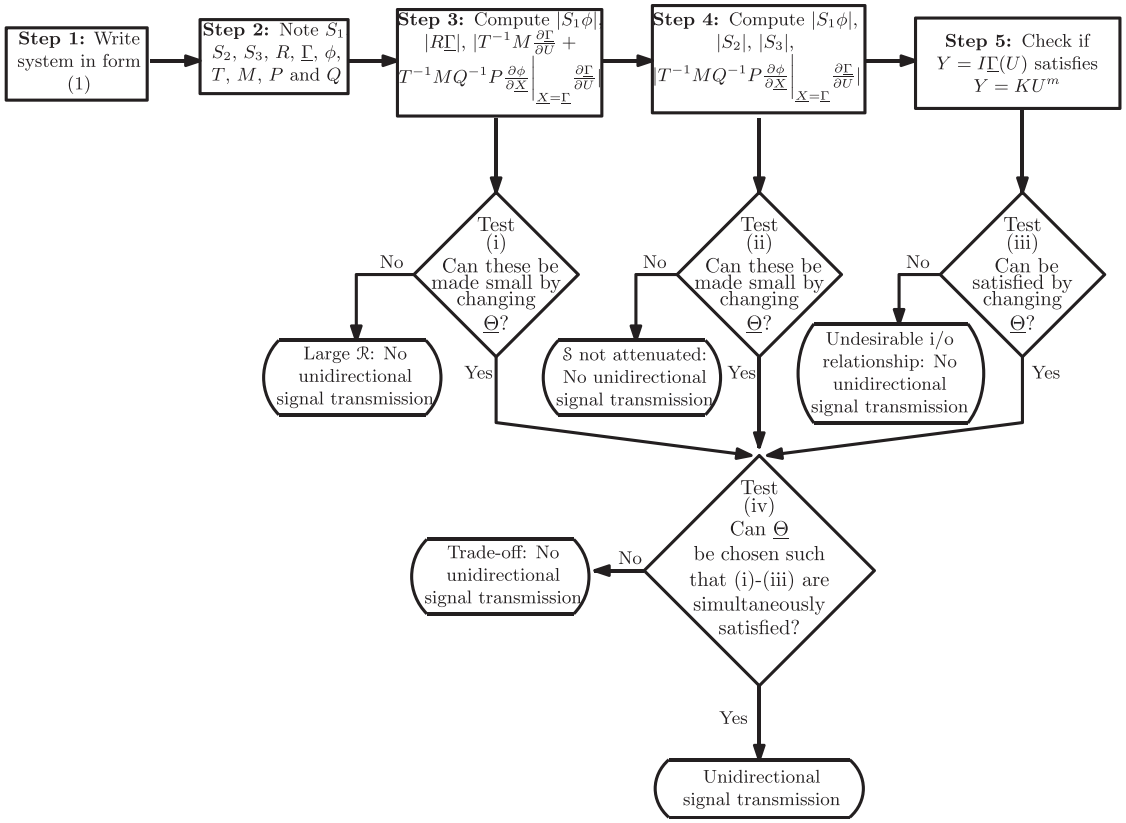

FIGURE 3 Procedure to determine whether a given signaling system satisfies definition 1 for unidirectional signal transmission.

Example). Steps 1–5 for this system are shown in Supporting Material, Section 1.3. We find that to satisfy test (i), we must have small X_T. Further, to satisfy test (ii), we must have large X_T and M_T. Finally, computing $I\underline{\Gamma}$ from step 5, we find that the input-output relationship has $K \approx (k_1K_{m2}/k_2K_{m1})(X_T/M_T)$ with $m = 1$ when $K_{m1}, K_{m2} \gg 1$. These results are consistent with those described in Example, as well as with previous theoretical and experimental work (8,11,33). There exists a tradeoff between requirements 1 and 2 of definition 1, i.e., between imparting a small retroactivity to the input and attenuating retroactivity to the output. Thus, $\underline{\mathbf{\Theta}}$ cannot be chosen such that all three requirements are simultaneously satisfied. Test (iv) fails, and the single PD cycle cannot achieve unidirectional signal transmission.

This way, the above procedure can be used to identify ways to tune the total protein concentration of a signaling system such that it satisfies definition 1. Using this procedure, we analyze a number of signaling architectures, including double phosphorylation systems, phosphotransfer systems, and multistage signaling architectures composed of these. For these architectures, we consider two types of input signals: a kinase input (highly represented in natural systems), where the input regulates the rate of phosphorylation, and a substrate input (less frequent in natural systems), where the input regulates the rate of production of the substrate.

Double phosphorylation cycle with input as kinase

Here, we consider a double phosphorylation cycle with a common kinase Z for both phosphorylation cycles as the input and the doubly phosphorylated substrate X^{**} as the output. This architecture is found in the second and third stages of the MAPK cascade, where the kinase phosphorylates both the threonine and tyrosine sites in a distributive process (44). This configuration is shown in Fig. 4 *A*. Referring to Fig. 1 *A*, the input signal U is the concentration Z of the kinase and the output signal Y is the concentration X^{**} of the doubly phosphorylated substrate X.

The input kinase is produced at a time-varying rate, $k(t)$. All species dilute with a rate constant δ, and the total promoter concentration in the downstream system is p_T. The total substrate and phosphatase concentrations are X_T and M_T, respectively. The Michaelis-Menten constants for the two phosphorylation and the two dephosphorylation reactions are K_{m1}, K_{m3}, K_{m2}, and K_{m4}, respectively. The catalytic reaction rate constants of these reactions are k_1, k_2, k_3, and k_4, respectively. The system's chemical reactions are shown in Supporting Material, Eq. 28. As explained before, the

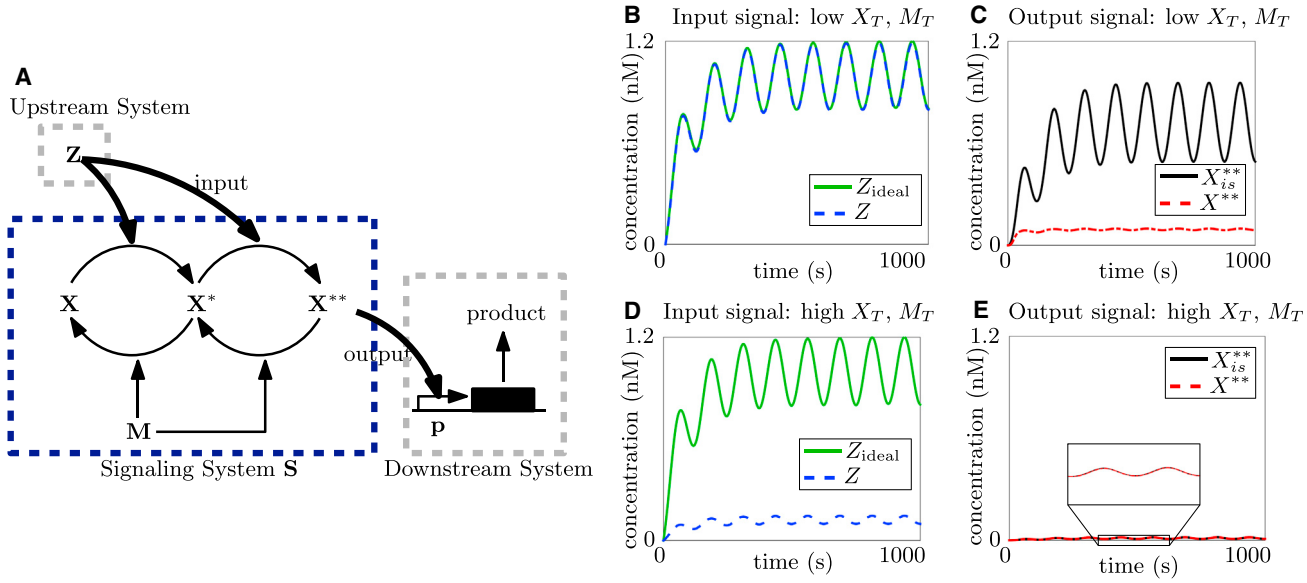

FIGURE 4 Tradeoff between small retroactivity to the input and attenuation of retroactivity to the output in a double phosphorylation cycle. (*A*) Double phosphorylation cycle, with input *Z* as the kinase: *X* is phosphorylated by Z to *X**, and further on to *X***. Both of these are dephosphorylated by the phosphatase *M*. *X*** is the output and acts on sites *p* in the downstream system, which is depicted as a gene expression system here. (*B–E*) Simulation results for the ODE model shown in Supporting Material, Eq. 29. Simulation parameters are given in Table S1. The ideal system is simulated for Z_{ideal} with $X_{\text{T}} = M_{\text{T}} = p_{\text{T}} = 0$. The isolated system for X^*_{is} is simulated with $p_{\text{T}} = 0$. To see this figure in color, go online.

parameters that we tune to investigate retroactivity effects are the total protein concentrations of the phosphorylation cycle, that is, X_{T} and M_{T}. Specifically, using the procedure in Fig. 3, we tune X_T and M_T to verify if this system can transmit a unidirectional signal, according to definition 1. Steps 1–5 are detailed in Supporting Material, Section 1.4. We therefore find the following.

1. Retroactivity to the input: Evaluating the terms in step 3, we find that to satisfy test (i), we must have small (X_{T}/K_{m1}) and small $(X_{\text{T}}/M_{\text{T}}K_{m3})(k_1K_{m2}/k_2K_{m1})$. Thus, to have small retroactivity to the input, the parameter X_{T} must be small. (Evaluation of terms in step 3 is shown in Supporting Material, Section 1.4).
2. Retroactivity to the output: Evaluating the terms in step 4, we find that to satisfy test (ii), we must have small $(p_{\text{T}}/X_{\text{T}})$ and $(\delta p_{\text{T}}/a_4M_{\text{T}})$. Thus, to attenuate retroactivity to the output, we must have large X_{T} and M_{T}. (Evaluation of terms in step 4 is shown in Supporting Material, Section 1.4).

(iii) Input-output relationship: Computing $I\underline{\Gamma}$ shows that $X^{**}_{\text{is}} \approx (k_1k_3K_{m2}K_{m4}/k_2k_4K_{m1}K_{m3})(X_{\text{T}}/M^2_{\text{T}})Z^2_{\text{is}}$ when $K_{m1},\ K_{m2},\ K_{m3},\ K_{m4} \gg Z_{\text{is}},\ K_{m2} \gg X^*_{\text{is}},\ K_{m4} \gg X^{**}_{\text{is}}$ and $M_{\text{T}} \gg Z_{\text{is}}$. Under these assumptions, this system satisfies test (iii) by tuning the ratio $(X_{\text{T}}/M^2_{\text{T}})$ to achieve a desired K with $m = 2$. (Evaluation of step 5 is shown in Supporting Material, Section 1.4).

This system shows opposing requirements to satisfy tests (i) and (ii), similar to the single phosphorylation cycle. Thus, although each of the requirements of tests (i)-(iii) are individually satisfied, the system does not satisfy test (iv), showing a tradeoff that prevents unidirectional signal transmission. Retroactivity to the input is large when substrate concentration X_{T} (and M_{T}) increases, because the input *Z* must phosphorylate a large amount of substrate, thus leading to a large reaction flux to Z due to the phosphorylation reaction. However, if X_{T} (and M_{T}) is made small, the system cannot attenuate the retroactivity to the output, since as the output *X*** is sequestered by the downstream system, there is not enough substrate available for the signaling system. Therefore, tests (i) and (ii) cannot be independently satisfied.

These mathematical predictions can be appreciated from the numerical simulations of Fig. 4, *B–E*, with a time-varying input, and from the simulations in Fig. S2, *B–E*, with a step input. This result is summarized in Fig. 9 *B*.

Regulated autophosphorylation followed by phosphotransfer

We now consider a signaling system composed of a phosphotransfer system, whose phosphate donor receives the phosphate group via autophosphorylation regulated by protein *Z*. An instance of this architecture is found in the bacterial chemotaxis network, where the autophosphorylation of protein CheA is regulated by a transmembrane receptor (e.g., Tar). CheA then transfers the phosphate group to protein CheY in a phosphotransfer reaction. CheY further undergoes dephosphorylation catalyzed by the phosphatase

CheZ (45–47). A similar mechanism is also present in the ubiquitous two-component signaling networks, where the sensor protein autophosphorylates upon binding to a stimulus (e.g., a ligand) and then transfers the phosphate group to the receptor protein (15,48). We model this regulated autophosphorylation as a phosphorylation reaction with kinase as input, since in both cases, first an intermediate complex is formed and the protein then undergoes phosphorylation. This architecture is shown in Fig. 5 *A*. In this case, the input signal U of Fig. 1 *A* is Z, which is the concentration of the kinase/stimulus Z that regulates the phosphorylation of the phosphate donor X_1, which then transfers the phosphate group to protein X_2. The output signal Y in Fig. 1 *A* is then X_2^*, which is the concentration of the phosphorylated substrate X_2^*. Protein X_2^* is dephosphorylated by phosphatase M. Total concentrations of proteins X_1, X_2, and M are X_{T1}, X_{T2}, and M_T, respectively. The Michaelis-Menten constants for the phosphorylation of X_1 by Z and dephosphorylation of X_2^* by M are K_{m1} and K_{m3}, and the catalytic rate constants of these are k_1 and k_3, respectively. The association rate constant of complex formation by X_2^* and X_1 is a_3. These reactions are shown in Supporting Material, Eq. 48. The total concentration of promoter sites in the downstream system is p_T. The input Z is produced at a time-varying rate, $k(t)$. As before, the parameters we change to analyze the system for unidirectional signal transmission are its total protein concentrations, X_{T1}, X_{T2}, and M_T. Using the procedure in Fig. 3, we analyze the system's ability to transmit unidirectional signals as per definition 1 as X_{T1}, X_{T2}, and M_T are varied. This is done as follows. (Steps 1–5 for this system are shown in Supporting Material, Section 1.5).

1. Retroactivity to the input: Evaluating the terms in step 3, we find that to satisfy test (i), we must have small (X_{T1}/K_{m1}). Thus, for small retroactivity to the input, we must have small X_{T1}. (Evaluation of the terms in step 3 is shown in Supporting Material, Section 1.5).
2. Retroactivity to the output: Evaluating the terms in step 4, we find that to satisfy test (ii), (p_T/X_{T2}) and $(\delta p_T/a_3 X_{T1})$ must be small. Thus, for a small retroactivity to the output, we must have large X_{T1} and X_{T2}. (Evaluation of terms in step 4 is shown in Supporting Material, Section 1.5).
3. Input-output relationship: Evaluating $I\underline{\Gamma}$ as in step 5, we find that $X_2^* \approx (k_1 K_{m3}/k_3 K_{m1})(X_{T1}/M_T)Z$ when $K_{m1} \gg Z_{is}$ and $K_{m4} \gg X_{2,is}^*$. Under these assumptions, this system satisfies test (iii), where a desired K can be achieved by tuning the ratio (X_{T1}/M_T) with $m = 1$. (Evaluation of step 5 is shown in Supporting Material, Section 1.5).

In light of findings 1 and 2, above, we note that tests (i) and (ii) cannot be simultaneously satisfied. Test (iv) fails, and the system shows a tradeoff in attenuating retroactivity to the input and output. Retroactivity to the input can be made small by making X_{T1} (and M_T) small, since kinase Z must phosphorylate less substrate. However, the system with low X_{T1} is unable to attenuate retroactivity to the output, which requires that X_{T1} be large. This is because, as the output X_2^* is sequestered by the downstream system and undergoes decay as a complex, this acts as an additional channel of removal for the phosphate group from the system, which was received from X_1^*. If X_{T1} (and M_T) is small,

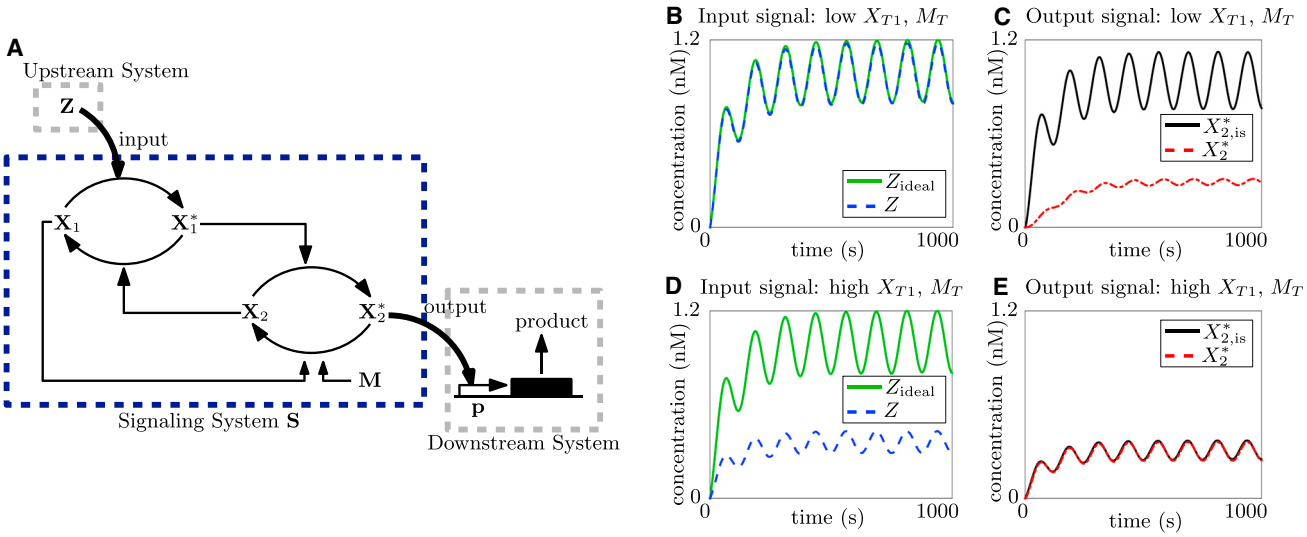

FIGURE 5 Tradeoff between small retroactivity to the input and attenuation of retroactivity to the output in a phosphotransfer system. (*A*) System with phosphorylation followed by phosphotransfer, with input Z as the kinase: Z phosphorylates X_1 to X_1^*. The phosphate group is transferred from X_1^* to X_2 by a phosphotransfer reaction, forming X_2^*, which is in turn dephosphorylated by the phosphatase M. X_2^* is the output and acts on sites p in the downstream system, which is depicted as a gene expression system here. (*B–E*) Simulation results for ODE (49) in Supporting Material, Section 1.5. Simulation parameters are given in Table S1. The ideal system is simulated for Z_{ideal} with $X_{T1} = X_{T2} = M_T = p_T = 0$. The isolated system is simulated for $X_{2,is}^*$ with $p_T = 0$. To see this figure in color, go online.

this removal of the phosphate group affects the amount of X_1^* in the system to a larger extent than when X_{T1} is large. Thus, there exists a tradeoff between requirements 1 and 2 of definition 1, and the system does not allow unidirectional signal transmission.

This mathematical analysis is demonstrated in the simulation results shown in Fig. 5, *B–E* with a time-varying input, and in the simulation results in Fig. S3, *B–E* with a step input. The discussion is further summarized in Fig. 9 *B*.

Cascade of single phosphorylation cycles

We have now seen three systems that show a tradeoff between attenuating retroactivity to the output and imparting a small retroactivity to the input: the single phosphorylation cycle, the double phosphorylation cycle, and the phosphotransfer system, all with a kinase as input. In all three cases, the tradeoff is due to the fact that, as the total substrate concentration is increased to attenuate the effect of retroactivity on the output, the system applies a large retroactivity to the input. Thus, requirements 1 and 2 of definition 1 cannot be independently achieved. In (34), a cascade of phosphotransfer systems was found to apply a small retroactivity to the input and to attenuate retroactivity to the output. Further, cascades of single and double PD cycles are ubiquitous in cellular signaling, such as in the MAPK cascade (14,49). The two-component signaling system (Regulated autophosphorylation followed by phosphotransfer) is also often the first stage of a cascade of signaling reactions (15,48). Motivated by this, here we consider a cascade of PD cycles to determine how a cascaded architecture can overcome this tradeoff. We have found that single and double PD cycles, and the phosphotransfer system, show similar properties with respect to unidirectional signal transmission. Thus, our findings are applicable to all systems composed of cascades of single-stage systems, such as the single PD cycle, the double PD cycle, and the phosphotransfer system analyzed in Regulated autophosphorylation followed by phosphotransfer (simulation results for cascades of different systems are shown in Figs. S15 and S16).

We consider a cascade of two single phosphorylation cycles, shown in Fig. 6 *A*. The input signal is Z, the concentration of kinase Z. Z phosphorylates substrate X_1 to X_1^*, which acts as a kinase for substrate X_2, phosphorylating it to X_2^*. X_1^* and X_2^* are dephosphorylated by phosphatases M_1 and M_2, respectively. The output signal is X_2^*, the concentration of X_2^*.

The input Z is produced at a time-varying rate, $k(t)$, and all species dilute with rate constant δ. The substrates of the cycles are produced at constant rates k_{X1} and k_{X2}, respectively, and the phosphatases are produced at constant rates k_{M1} and k_{M2}. We then define $X_{T1} = (k_{X1}/\delta)$, $X_{T2} = (k_{X2}/\delta)$, $M_{T1} = (k_{M2}/\delta)$, and $M_{T2} = (k_{M2}/\delta)$. The concentration of promoter sites in the downstream system is p_T. The Michaelis-Menten constants for the phosphorylation and dephosphorylation reactions are K_{m1}, K_{m3}, K_{m2}, and K_{m4}, respectively, and catalytic rate constants are k_1, k_3, k_2, and k_4. The chemical reactions for this system are shown in Supporting Material, Eq. 58. As before, the parameters we vary to analyze this system's ability to transmit unidirectional signals are X_{T1}, X_{T2}, M_{T1}, and M_{T2}. Using the procedure in Fig. 3, we seek to tune these to satisfy the requirements of definition 1. We find the following. (Steps 1–5 are detailed in Supporting Material, Section 1.6.)

1. Retroactivity to the input: Evaluating the terms in step 3, we find that to satisfy test (i), (X_{T1}/K_{m1}) must be small. Thus, to have a small retroactivity to the input, X_{T1} must be small. (Evaluation of terms in step 3 is shown in Supporting Material, Section 1.6.)
2. Retroactivity to the output: As before, we evaluate the terms in step 4, and find that to satisfy test (ii), we must have small (p_T/X_{T2}) and $(\delta p_T/a_4 M_{T2})$. Thus, to attenuate retroactivity to the output, M_{T2} and X_{T2} must

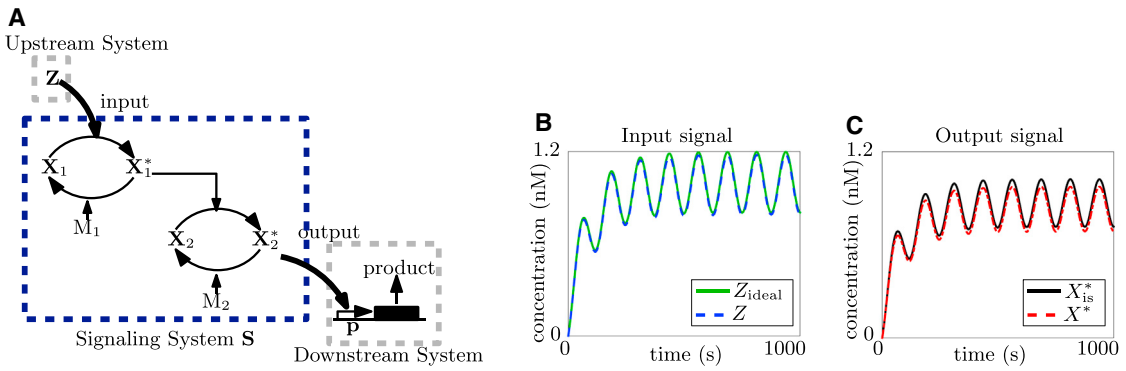

FIGURE 6 Tradeoff between small retroactivity to the input and attenuation of retroactivity to the output is overcome by a cascade of single phosphorylation cycles. (*A*) Cascade of two phosphorylation cycles, with kinase Z as the input: Z phosphorylates X_1 to X_1^*, X_1^* acts as the kinase for X_2, phosphorylating it to X_2^*, which is the output, acting on sites p in the downstream system, which is depicted as a gene expression system here. X_1^* and X_2^* are dephosphorylated by phosphatases M_1 and M_2, respectively. (*B* and *C*) Simulation results for ODEs in Supporting Material, Eqs. 72–79, with $N = 2$. Simulation parameters are given in Table S1. The ideal system is simulated for Z_{ideal} with $X_{T1} = X_{T2} = M_T = p_T = 0$. The isolated system is simulated for $X^*_{2,is}$ with $p_T = 0$. To see this figure in color, go online.

be large. (Evaluation of terms in step 4 is shown in Supporting Material, Section 1.6.)

3. Input-output relationship: Evaluating $I\underline{\Gamma}$ as in step 5, we find that the input-output relationship is $X^*_{2,\mathrm{is}} \approx (k_1k_3K_{m2}K_{m4}/k_2k_4K_{m1}K_{m3})(X_{\mathrm{T1}}X_{\mathrm{T2}}/M_{\mathrm{T1}}M_{\mathrm{T2}})Z_{\mathrm{is}}$ when K_{m1}, K_{m2}, K_{m3}, $K_{m4} \gg Z_{\mathrm{is}}$ and $M_{\mathrm{T2}} \ll K_{m4}$. (Details are shown in Supporting Material, Section 1.6.) The ratio $(X_{\mathrm{T1}}X_{\mathrm{T2}}/M_{\mathrm{T1}}M_{\mathrm{T2}})$ can thus be tuned such that the system satisfies test (iii) with $m = 1$. However, if the different stages of the cycle share a common phosphatase, additional cycles may be required to maintain a linear input-output response (50). Details of this analysis are shown in step 5 of Supporting Material, Section 1.7.

Finally, we see that test (iv) is satisfied for this system, since tests (i)–(iii) can be satisfied simultaneously. We thus note that the tradeoff between attenuating retroactivity to the output and imparting small retroactivity to the input, found in single-stage systems, is broken by having a cascade of two cycles. This is because the input kinase Z only directly interacts with the first cycle, and thus, when X_{T1} is made small, the upstream system faces a small reaction flux due to the phosphorylation reaction, making retroactivity to the input small. The downstream system sequesters the species X^*_2, and when X_{T2} is made high, there is enough substrate X_2 available for the signaling system to be nearly unaffected, thus attenuating retroactivity to the output. This is verified in Fig. 6, *B* and *C*. The tradeoff found in the single cycle in Fig. 2, *B–E*, is overcome by the cascade, where we have tuned M_{T1} and M_{T2} to satisfy requirement 3 of definition 1. When the total substrate concentration for a single cycle is low, the retroactivity to the input is small (Fig. 2 *B*), but the retroactivity to the output is not attenuated (Fig. 2 *C*). When the total substrate concentration of this cycle is increased, the retroactivity to the output is attenuated (Fig. 2 *D*), but the input, and therefore the output, is highly changed due to an increase in the retroactivity to the input (Fig. 2, *D* and *E*). When the same two cycles are cascaded, with the low substrate concentration cycle being the first and the high substrate concentration cycle being the second (and M_{T1} and M_{T2} tuned to maintain the same gain K as the single cycles), retroactivity to the input is small and retroactivity to the output is attenuated (Fig. 6, *B* and *C*). Thus, cascading two cycles overcomes the tradeoff found in a single cycle. The same conclusions can also be appreciated from the simulation results for a step-input response in Fig. S1.

These results are summarized in Fig. 9 *E*. Although the system demonstrated here is a cascade of single phosphorylation cycles, the same decoupling is true for cascaded systems composed of double phosphorylation cycles and phosphorylation cycles followed by phosphotransfer, which, as we saw in the previous subsections, show a similar kind of tradeoff. Cascades of such systems, with the first system with a low substrate concentration and the last system with a high substrate concentration thus both impart a small retroactivity to the input and attenuate retroactivity to the output and are therefore able to transmit unidirectional signals. This can be seen via simulation results in Supporting Material, Section 1.7.1, where a cascade of a phosphotransfer system and a single PD cycle is seen in Fig. S5 and a cascade of a single PD cycle and a double PD cycle is seen in Fig. S6.

Phosphotransfer with the phosphate donor undergoing autophosphorylation as input

Here, we consider a signaling system composed of a protein X_1 that undergoes autophosphorylation and then transfers the phosphate group to a substrate X_2, shown in Fig. 7 *A*. In Regulated autophosphorylation followed by phosphotransfer, we considered a system with regulated autophosphorylation, where the input is a ligand/kinase. In this section, motivated by proteins that undergo autophosphorylation and then transfer the phosphate group, we consider a system where the input is the protein undergoing autophosphorylation (substrate input). Based on our literature review, we have not found instances of such systems in nature, and in this section, we investigate whether they might pose a disadvantage to unidirectional signaling. The input signal U of Fig. 1 *A* is X_1, the concentration of protein X_1 that undergoes autophosphorylation, and the output signal Y of Fig. 1 *A* is X^*_2, the concentration of phosphorylated protein X^*_2. The total protein concentrations of substrate X_2 and phosphatase M are X_{T2} and M_{T}, respectively. The total concentration of promoters in the downstream system is p_{T}. Autophosphorylation of a protein typically follows a conformational change that either allows the protein to dimerize and phosphorylate itself or stimulates the phosphorylation of the monomer (51). Here, we model the latter mechanism for autophosphorylation as a single step with rate constant π_1. The Michaelis-Menten constant for the dephosphorylation of X^*_2 by M is K_{m3}, and the association, dissociation, and catalytic rate constants for this reaction are a_3, d_3, and k_3. The association and dissociation rate constants for the complex formed by X^*_1 and X_2 are a_1 and d_1, the dissociation rate constant of this complex into X_1 and X^*_2 is d_2, and the corresponding reverse association rate constant is a_2. The input protein X_1 is produced at a time-varying rate, $k(t)$. Details of the chemical reactions of this system are shown in Supporting Material, Eq. 101. We use the procedure in Fig. 3 to analyze this system as per definition 1 by varying the total protein concentrations X_{T2} and M_{T}. This is done as follows. (Steps 1–5 are detailed in Supporting Material, Section 1.8.)

1. Retroactivity to input: Evaluating the terms in step 3, we find that to satisfy test (i), $(2d_1a_2K/a_1d_2X_{\mathrm{T2}})$, $(\pi_1(d_1 + d_2)/a_1d_2X_{\mathrm{T2}})$, $(2a_2K/d_2)$, and (π_1/d_2) must be small, where $K = (\pi_1K_{m3}/k_3M_{\mathrm{T}})$. However, not all these terms can be made smaller by varying X_{T2} and M_{T} alone. Thus, the retroactivity to the input, and

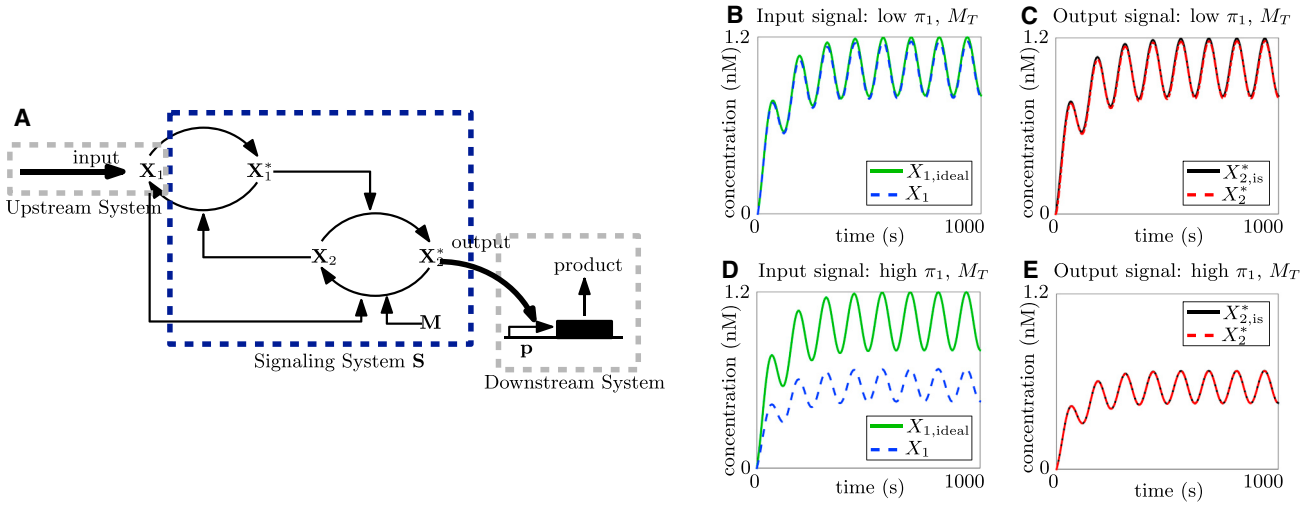

FIGURE 7 Attenuation of retroactivity to the output by a phosphotransfer system. (*A*) System with autophosphorylation followed by phosphotransfer, with input as protein X_1 which autophosphorylates to X_1^*. The phosphate group is transferred from X_1^* to X_2 by a phosphotransfer reaction, forming X_2^*, which is in turn dephosphorylated by the phosphatase M. X_2^* is the output and acts on sites p in the downstream system, which is depicted as a gene expression system here. (*B–E*) Simulation results for the ODE in Supporting Material, Eq. 102. Simulation parameters are given in Table S1. The ideal system is simulated for $X_{1,\text{ideal}}$ with $X_{T2} = M_T = \pi_1 = p_T = 0$. The isolated system is simulated for $X_{2,\text{is}}^*$ with $p_T = 0$. To see this figure in color, go online.

whether or not test (i) is satisfied, depends on the reaction rate constants of the system, and it is not possible to tune it using total protein concentrations alone. (Evaluation of terms in step 3 is shown in Supporting Material, Section 1.8.)

2. Retroactivity to output: Evaluating the terms in step 4, we find that to satisfy test (ii), we must have a small (p_T/X_{T2}) and $(p_T\delta/a_3M_T)$. Thus, to attenuate retroactivity to the output, X_{T2} and M_T must be large. (Evaluation of terms in step 4 is shown in Supporting Material, Section 1.8.)
3. Input-output relationship: Evaluating $I\underline{\Gamma}$ as in step 5, we find that the input-output relationship is $X_{2,\text{is}}^* \approx (\pi_1 K_{m3}/k_3 M_T)X_{1,\text{is}}$ when $K_{m3} \gg X_{2,\text{is}}^*$ and thus, this system can satisfy test (iii) by tuning M_T to achieve a desired K with $m = 1$. (Details of step 5 are shown in Supporting Material, Section 1.8.)

Thus, we find that the retroactivity to the input cannot be made small by changing concentrations alone. The retroactivity to the output can be attenuated by having a large X_{T2} and M_T, since these can compensate for the sequestration of X_2^* by the downstream system. This signaling system can therefore satisfy tests (ii) and (iii) for unidirectional signal transmission. Although satisfying these requirements does not increase the retroactivity to the input, thus making it possible for it to satisfy test (i) as well, retroactivity to the input depends on the reaction-rate parameters, in particular, on the forward reaction-rate constant, π_1, of autophosphorylation of X_1. If this is large, the autophosphorylation reaction applies a large reaction flux to the upstream system, thus resulting in a large retroactivity to the input. If π_1 is small, this flux is small, and thus, retroactivity to the input is small. By the way we have defined cascades (as signals between stages transmitted through a kinase), any cascade containing this system would have it as a first stage. Therefore, even cascading this system with different architectures would not overcome the above limitation. These mathematical predictions can be appreciated in the simulation results shown in Fig. 7, *B–E* for a time-varying input, and in the simulation results shown in Fig. S7, *B–E* with a step input. The result is summarized in Fig. 9 *C*.

Single cycle with substrate input

Here, we consider a single phosphorylation cycle where the input signal U of Fig. 1 *A* is X, the concentration of the substrate X, and the output signal Y is X^*, the concentration of the phosphorylated substrate. We consider this system motivated by the various transcription factors that undergo phosphorylation before activating or repressing their targets, such as the transcriptional activator nitrogen regulator I in the *Escherichia coli* nitrogen assimilation system (52). However, to the best of our knowledge, based on our literature review, signals are more commonly transmitted through kinases, as opposed to being transmitted by the substrates of phosphorylations. Since these are less represented than the others in natural systems, we ask whether they have any disadvantage for unidirectional transmission, and in fact they do. Note that the system analyzed in Phosphotransfer with the phosphate donor undergoing autophosphorylation as input is a system that takes as input a kinase that undergoes autophosphorylation before donating the phosphate group, and is not the same as the system considered here, where the input is a substrate of enzymatic phosphorylation.

The signaling system we consider, along with the upstream and downstream systems, is shown in Fig. 8 *A*. The input protein X is produced at a time-varying rate, $k(t)$. It is phosphorylated by kinase Z to the output protein X^*, which is in turn dephosphorylated by phosphatase M. X^* then acts as a transcription factor for the promoter sites in the downstream system. All the species in the system decay with rate constant δ. The total concentration of promoters in the downstream system is p_T. The total kinase and phosphatase concentrations are Z_T and M_T, respectively, which are the parameters of the system we vary. The Michaelis-Menten constants of the phosphorylation and dephosphorylation reactions are K_{m1} and K_{m2}, and the catalytic rate constants are k_1 and k_2. The chemical reactions of this system are shown in Supporting Material, Eq. 112. Using the procedure in Fig. 3, we analyze whether this system can transmit a unidirectional signal according to definition 1 by varying Z_T and M_T. This is done as follows (steps 1–5 in Supporting Material, Section 1.9).

1. Retroactivity to the input: Evaluating the terms in step 3, we find that they cannot be made small by changing Z_T and M_T, and therefore, test (i) fails and retroactivity to the input cannot be made small. (Evaluation of terms in step 3 is shown in Supporting Material, Section 1.9).
2. Retroactivity to the output: Similarly, we evaluate the terms in step 4 and find that they cannot be made small by varying Z_T and M_T. Thus, test (ii) fails and retroactivity to the output cannot be attenuated by tuning these parameters. (Evaluation of terms in step 4 is shown in Supporting Material, Section 1.9.)
3. Input-output relationship: Evaluating $I\underline{\Gamma}$ as in step 5, we find that the input-output relationship is linear with gain $K = (((k_1 Z_T/K_{m1})/(k_2 M_T/K_{m2}) + \delta))$ when $K_{m1}, K_{m2} \gg X$, that is:

$$X^*_{is}(t) \approx K X_{is}(t). \tag{5}$$

The input-output relationship is thus linear, i.e., $m = 1$, and K can be tuned by varying Z_T and M_T. The system thus satisfies test (iii). (Details of step 5 are shown in Supporting Material, Section 1.9.)

Thus, we find that a signaling system composed of a single phosphorylation cycle with substrate as input cannot transmit a unidirectional signal, since it can neither make retroactivity to the input small nor attenuate retroactivity to the output. This is because the same protein X is the input (when unmodified) and the output (when phosphorylated). Thus, when X undergoes phosphorylation, the concentration of input X is reduced by conversion to X^*, thus applying a large retroactivity to the input. Now, when X^* is sequestered by the downstream system, this results in a large flux to both X and X^*, and thus the retroactivity to the output is also large. In fact, the same is true for an architecture with the input undergoing double phosphorylation, as seen in Supporting Material, Section 1.10, where X^{**} is the output. For this architecture, as X^{**} is sequestered, this applies a large flux to X, X^*, and X^{**}. Cascading such systems would also not enhance their ability to transmit unidirectional signals: if the system were used as the first stage to a cascade, it would apply a large retroactivity to the input for the aforementioned reasons. The way we have defined cascades

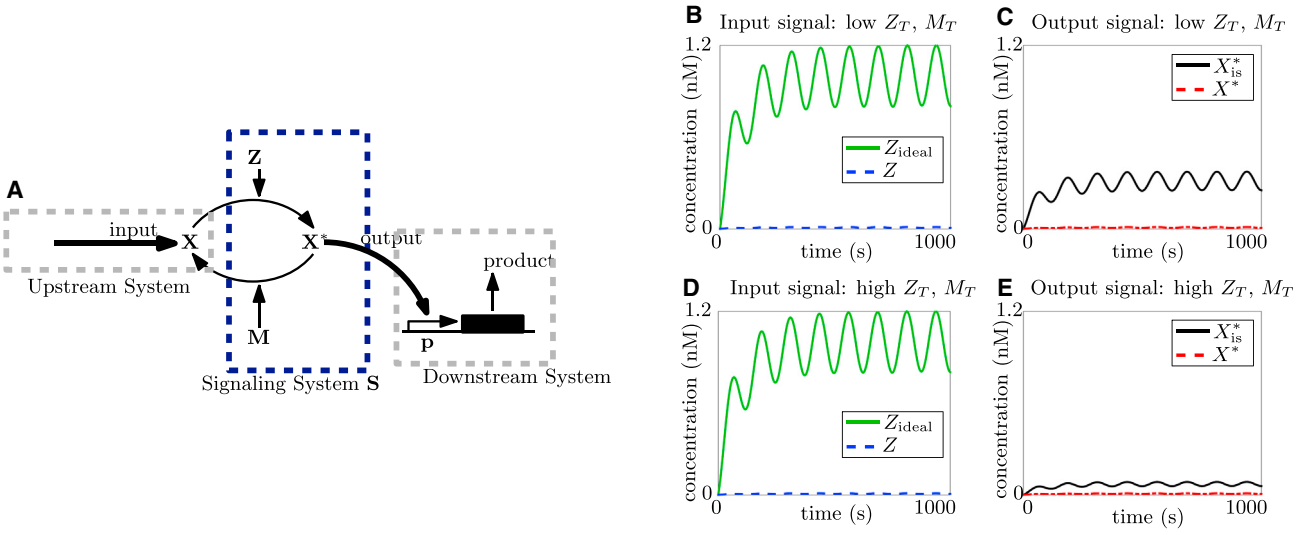

FIGURE 8 Inability to attenuate retroactivity to the output or impart small retroactivity to the input by a single phosphorylation cycle with substrate as input. (*A*) Single phosphorylation cycle, with input X as the substrate: X is phosphorylated by the kinase Z to X^*, which is dephosphorylated by the phosphatase M back to X. X^* is the output and acts as a transcription factor for the promoter sites p in the downstream system. (*B–E*) Simulation results for the ODEs in Supporting Material, Eqs. 113 and 114. Simulation parameters are given in Table S1. The ideal system is simulated for X_{ideal} with $X_T = M_T = p_T = 0$. The isolated system is simulated for X^*_{is} with $p_T = 0$. To see this figure in color, go online.

above, with noninitial stages receiving their input via a kinase, this system cannot be the second stage of a cascade, since it takes its input in the form of the substrate. These results are demonstrated in the simulation results shown in Fig. 8, *B–E*, for a sinusoidal input, and in Figs. S18, *B–E*, for a step input. Results for the double phosphorylation cycle with substrate input are seen from Figs. S19 and S20. These results are summarized in Fig. 9 *F*.

DISCUSSION

Retroactivity effects have been shown to be useful in certain contexts, such as transcription-factor decoy sites that convert graded dose responses to sharper, more switch-like responses (53). However, retroactivity is one of the chief hurdles to one-way transmission of information (8–13). The goal of this work was to identify signaling architectures that can overcome retroactivity and thus allow the transmission of unidirectional signals. To achieve this, we have provided a procedure that can be used to analyze any signaling system composed of reactions such as PD and phosphotransfer. We have then considered different signaling architectures (Fig. 9) and have used this procedure to determine whether they have the ability to minimize retroactivity to the input and attenuate retroactivity to the output.

We have found that a main discriminating factor is whether the signaling architecture transmits information from kinases or from substrates. Specifically, phosphorylation cycles (single or double) and phosphotransfer systems that transmit information from an input kinase (Fig. 9, *A–C*) show a tradeoff between minimizing retroactivity to the input and attenuating retroactivity to the output, consistent with prior experimental studies (33,54). Yet cascades of such systems (see, for example Fig. 9 *E*) can break this tradeoff. This is achieved when the first stage has low substrate concentration, thus imparting a small retroactivity to the input, and the last stage has high substrate concentration, thus attenuating retroactivity to the output. Interestingly, this low-high substrate concentration pattern appears in the MAPK signaling cascade in the mature *Xenopus* oocyte, where the first stage is a phosphorylation cycle with substrate concentration in the nanomolar range and the last two stages are double phosphorylation cycle with substrate concentration in the thousands of nanomoles (25). This low-high pattern indicates an ability to overcome retroactivity and transmit unidirectional signals, and although this structure may serve other purposes as well, it is possible that the substrate concentration pattern has evolved to more efficiently transmit unidirectional signals. By contrast, architectures that transmit information from a substrate (Fig. 9, *D–G*) do not perform as well even when cascaded. Consistent with this finding, whereas architectures that transmit signals from an input kinase are highly represented in cellular signaling, such as in the MAPK cascade and two-component signaling (1–7,16–19), those receiving signals

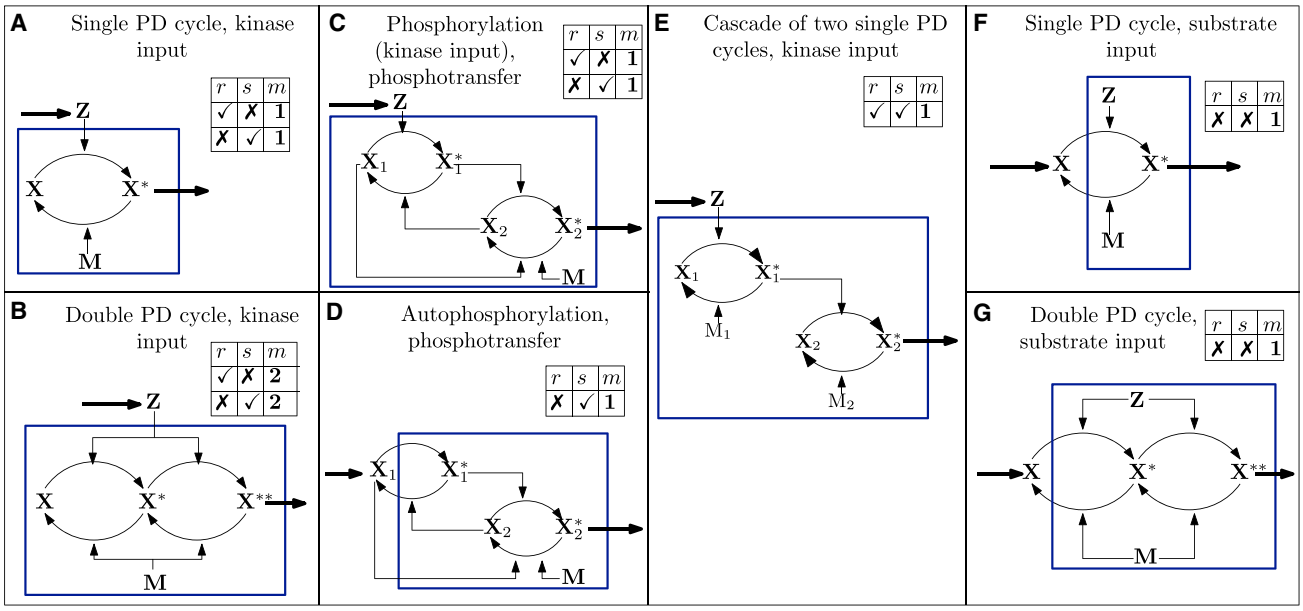

FIGURE 9 Table summarizing the results. For each inset table, a ✓(✗) for column r implies that the system can (cannot) be designed to minimize retroactivity to the input by varying total protein concentrations, a ✓(✗) for column s implies that the system can (cannot) be designed to attenuate retroactivity to the output by varying total protein concentrations, and column m describes the input-output relationship of the system (i.e., $Y \approx KU^m$) as described in definition 1, requirement 3). Thus, as seen above, systems (D), (F), and (G) fail to satisfy at least one of the three requirements for definition 1 for unidirectional signaling. Inset tables with two rows imply that one of the two rows can be achieved for a set of values for the design parameters: thus, the two rows for systems (*A*)–(*C*) show the tradeoff between the ability to minimize retroactivity to the input (*first row*) and the ability to attenuate retroactivity to the output (*second row*). Note that this tradeoff is overcome by the cascade (*E*). To see this figure in color, go online.

through substrates are not as frequent in natural systems. This was in fact the reason we chose to analyze systems with substrate as input. We wished to determine whether they show a disadvantage to unidirectional signaling, potentially explaining why they are not frequently seen. It has also been reported that kinase-to-kinase relationships are highly conserved evolutionarily (55), implying that upon evolution, signaling mechanisms where kinases phosphorylate other kinases are conserved. These facts support the notion that cellular signaling has evolved to favor one-way transmission.

For graph-based methods for analyzing cellular networks (56), such as discovering functional modules based on motif search or clustering, signaling pathway architectures that transmit unidirectional signals can then be treated as directed edges. On the contrary, analysis of signaling systems (such as those with a substrate as input) that do not demonstrate the ability to transmit unidirectional signals must take into account the effects of retroactivity. These effects could result in cross talk between different targets of the signaling system, since a change in one target would affect the others by changing the signal being transmitted through the pathway (13). Our work provides a way to identify signaling architectures that overcome such effects and that can be treated as modules whose input/output behavior is largely independent from the context. Our findings further uncover a library of systems that transmit unidirectional signals, which could be used in synthetic biology to connect genetic components, enabling modular circuit design.

SUPPORTING MATERIAL

Supporting Materials and Methods, eleven figures, and nine tables are available at http://www.biophysj.org/biophysj/supplemental/S0006-3495(17)30669-0.

AUTHOR CONTRIBUTIONS

R.S. performed the research, developed the mathematical analysis, and wrote the article. D.D.V. designed the research, assisted with the mathematical analysis, and edited the article.

ACKNOWLEDGMENTS

This work was funded by the NSF Expedition award 1521925 and the NIGMS grant P50 GMO98792.

REFERENCES

1. Chang, F., J. T. Lee, …, J. A. McCubrey. 2003. Involvement of PI3K/Akt pathway in cell cycle progression, apoptosis, and neoplastic transformation: a target for cancer chemotherapy. *Leukemia.* 17:590–603.
2. Christian, F., E. L. Smith, and R. J. Carmody. 2016. The regulation of NF-κB subunits by phosphorylation. *Cells.* 5:12.
3. Garcia-Garcia, T., S. Poncet, …, M. F. Noirot-Gros. 2016. Role of protein phosphorylation in the regulation of cell cycle and DNA-related processes in bacteria. *Front. Microbiol.* 7:184.
4. Bonni, A., A. Brunet, …, M. E. Greenberg. 1999. Cell survival promoted by the Ras-MAPK signaling pathway by transcription-dependent and -independent mechanisms. *Science.* 286:1358–1362.
5. Hardie, D. G. 2004. The AMP-activated protein kinase pathway—new players upstream and downstream. *J. Cell Sci.* 117:5479–5487.
6. Hay, N., and N. Sonenberg. 2004. Upstream and downstream of mTOR. *Genes Dev.* 18:1926–1945.
7. Kolch, W. 2000. Meaningful relationships: the regulation of the Ras/Raf/MEK/ERK pathway by protein interactions. *Biochem. J.* 351:289–305.
8. Del Vecchio, D., A. J. Ninfa, and E. D. Sontag. 2008. Modular cell biology: retroactivity and insulation. *Mol. Syst. Biol.* 4:161.
9. Ventura, A. C., P. Jiang, …, A. J. Ninfa. 2010. Signaling properties of a covalent modification cycle are altered by a downstream target. *Proc. Natl. Acad. Sci. USA.* 107:10032–10037.
10. Jayanthi, S., K. S. Nilgiriwala, and D. Del Vecchio. 2013. Retroactivity controls the temporal dynamics of gene transcription. *ACS Synth. Biol.* 2:431–441.
11. Jiang, P., A. C. Ventura, …, D. Del Vecchio. 2011. Load-induced modulation of signal transduction networks. *Sci. Signal.* 4:ra67.
12. Kim, Y., Z. Paroush, …, S. Y. Shvartsman. 2011. Substrate-dependent control of MAPK phosphorylation in vivo. *Mol. Syst. Biol.* 7:467.
13. Kim, Y., M. Coppey, …, S. Y. Shvartsman. 2010. MAPK substrate competition integrates patterning signals in the *Drosophila* embryo. *Curr. Biol.* 20:446–451.
14. Robinson, M. J., and M. H. Cobb. 1997. Mitogen-activated protein kinase pathways. *Curr. Opin. Cell Biol.* 9:180–186.
15. Stock, A. M., V. L. Robinson, and P. N. Goudreau. 2000. Two-component signal transduction. *Annu. Rev. Biochem.* 69:183–215.
16. Sherr, C. J. 1996. Cancer cell cycles. *Science.* 274:1672–1677.
17. Lukas, J., C. Lukas, and J. Bartek. 2004. Mammalian cell cycle checkpoints: signalling pathways and their organization in space and time. *DNA Repair (Amst.).* 3:997–1007.
18. Senderowicz, A. M., and E. A. Sausville. 2000. Preclinical and clinical development of cyclin-dependent kinase modulators. *J. Natl. Cancer Inst.* 92:376–387.
19. DiPaola, R. S. 2002. To arrest or not to G_2-M cell-cycle arrest : commentary re: A. K. Tyagi et al., Silibinin strongly synergizes human prostate carcinoma DU145 cells to doxorubicin-induced growth inhibition, G_2-M arrest, and apoptosis. Clin. Cancer Res., 8: 3512–3519, 2002. *Clin. Cancer Res.* 8:3311–3314.
20. Stadtman, E. R., and P. B. Chock. 1977. Superiority of interconvertible enzyme cascades in metabolic regulation: analysis of monocyclic systems. *Proc. Natl. Acad. Sci. USA.* 74:2761–2765.
21. Chock, P. B., and E. R. Stadtman. 1980. Covalently interconvertible enzyme cascade systems. *Methods Enzymol.* 64:297–325.
22. Rhee, S. G., R. Park, …, E. R. Stadtman. 1978. Allosteric regulation of monocyclic interconvertible enzyme cascade systems: use of *Escherichia coli* glutamine synthetase as an experimental model. *Proc. Natl. Acad. Sci. USA.* 75:3138–3142.
23. Goldbeter, A., and D. E. Koshland, Jr. 1981. An amplified sensitivity arising from covalent modification in biological systems. *Proc. Natl. Acad. Sci. USA.* 78 (11):6840–6844.
24. Goldbeter, A., and D. E. Koshland, Jr. 1984. Ultrasensitivity in biochemical systems controlled by covalent modification. Interplay between zero-order and multistep effects. *J. Biol. Chem.* 259:14441–14447.
25. Huang, C. Y., and J. E. Ferrell, Jr. 1996. Ultrasensitivity in the mitogen-activated protein kinase cascade. *Proc. Natl. Acad. Sci. USA.* 93:10078–10083.
26. Sauro, H. M., and B. N. Kholodenko. 2004. Quantitative analysis of signaling networks. *Prog. Biophys. Mol. Biol.* 86:5–43.

27. Kholodenko, B. N. 2006. Cell-signalling dynamics in time and space. *Nat. Rev. Mol. Cell Biol.* 7:165–176.

28. Birtwistle, M. R., M. Hatakeyama, …, B. N. Kholodenko. 2007. Ligand-dependent responses of the ErbB signaling network: experimental and modeling analyses. *Mol. Syst. Biol.* 3:144.

29. Gomez-Uribe, C., G. C. Verghese, and L. A. Mirny. 2007. Operating regimes of signaling cycles: statics, dynamics, and noise filtering. *PLoS Comput. Biol.* 3:e246.

30. Mettetal, J. T., D. Muzzey, …, A. van Oudenaarden. 2008. The frequency dependence of osmo-adaptation in *Saccharomyces cerevisiae*. *Science.* 319:482–484.

31. Ventura, A. C., J.-A. Sepulchre, and S. D. Merajver. 2008. A hidden feedback in signaling cascades is revealed. *PLoS Comput. Biol.* 4 (3):e1000041.

32. Jayanthi, S., and D. Del Vecchio. 2011. Retroactivity attenuation in bio-molecular systems based on timescale separation. *IEEE Trans. Automat. Contr.* 56:748–761.

33. Nilgiriwala, K. S., J. Jiménez, …, D. Del Vecchio. 2015. Synthetic tunable amplifying buffer circuit in *E. coli*. *ACS Synth. Biol.* 4:577–584.

34. Mishra, D., P. M. Rivera, …, R. Weiss. 2014. A load driver device for engineering modularity in biological networks. *Nat. Biotechnol.* 32:1268–1275.

35. Ossareh, H. R., A. C. Ventura, …, D. Del Vecchio. 2011. Long signaling cascades tend to attenuate retroactivity. *Biophys. J.* 100:1617–1626.

36. Catozzi, S., J. P. Di-Bella, …, J. A. Sepulchre. 2016. Signaling cascades transmit information downstream and upstream but unlikely simultaneously. *BMC Syst. Biol.* 10:84.

37. McArthur, A. J., A. E. Hunt, and M. U. Gillette. 1997. Melatonin action and signal transduction in the rat suprachiasmatic circadian clock: activation of protein kinase C at dusk and dawn. *Endocrinology.* 138:627–634.

38. Schachtman, D. P., and R. Shin. 2007. Nutrient sensing and signaling: NPKS. *Annu. Rev. Plant Biol.* 58:47–69.

39. Golding, I., J. Paulsson, …, E. C. Cox. 2005. Real-time kinetics of gene activity in individual bacteria. *Cell.* 123:1025–1036.

40. Legewie, S., H. Herzel, …, N. Blüthgen. 2008. Recurrent design patterns in the feedback regulation of the mammalian signalling network. *Mol. Syst. Biol.* 4:190.

41. Dekel, E., and U. Alon. 2005. Optimality and evolutionary tuning of the expression level of a protein. *Nature.* 436:588–592.

42. Arpino, J. A., E. J. Hancock, …, K. Polizzi. 2013. Tuning the dials of synthetic biology. *Microbiology.* 159:1236–1253.

43. Karin, M. 1994. Signal transduction from the cell surface to the nucleus through the phosphorylation of transcription factors. *Curr. Opin. Cell Biol.* 6:415–424.

44. Markevich, N. I., J. B. Hoek, and B. N. Kholodenko. 2004. Signaling switches and bistability arising from multisite phosphorylation in protein kinase cascades. *J. Cell Biol.* 164:353–359.

45. Stewart, R. C. 1997. Kinetic characterization of phosphotransfer between CheA and CheY in the bacterial chemotaxis signal transduction pathway. *Biochemistry.* 36:2030–2040.

46. Bourret, R. B., J. Davagnino, and M. I. Simon. 1993. The carboxy-terminal portion of the CheA kinase mediates regulation of autophosphorylation by transducer and CheW. *J. Bacteriol.* 175:2097–2101.

47. Webre, D. J., P. M. Wolanin, and J. B. Stock. 2003. Bacterial chemotaxis. *Curr. Biol.* 13:R47–R49.

48. Perraud, A.-L., V. Weiss, and R. Gross. 1999. Signalling pathways in two-component phosphorelay systems. *Trends Microbiol.* 7:115–120.

49. Wilkinson, M. G., and J. B. Millar. 2000. Control of the eukaryotic cell cycle by MAP kinase signaling pathways. *FASEB J.* 14:2147–2157.

50. Shah, R., and D. Del Vecchio. 2016. An N-stage cascade of phosphorylation cycles as an insulation device for synthetic biological circuits. *In* Proceedings of the 2016 European Control Conference. ECC, pp. 1832–1837.

51. White, M. F., and C. R. Kahn. 1994. The insulin signaling system. *J. Biol. Chem.* 269:1–4.

52. Ninfa, A. J., L. J. Reitzer, and B. Magasanik. 1987. Initiation of transcription at the bacterial glnAp2 promoter by purified *E. coli* components is facilitated by enhancers. *Cell.* 50:1039–1046.

53. Lee, T. H., and N. Maheshri. 2012. A regulatory role for repeated decoy transcription factor binding sites in target gene expression. *Mol. Syst. Biol.* 8:576.

54. Rivera, P. M., and D. Del Vecchio. 2012. Optimal design of phosphorylation-based insulation devices. *In* Proceedings of the American Control Conference (ACC), 2013. IEEE, pp. 3783–3789.

55. Hu, J., H. Rho, …, J. Qian. 2014. Global analysis of phosphorylation networks in humans. *Biochim. Biophys. Acta.* 1844:224–231.

56. Aittokallio, T., and B. Schwikowski. 2006. Graph-based methods for analysing networks in cell biology. *Brief. Bioinform.* 7:243–255.